THE TRANSIENT RESPONSE AND IMPEDANCE LOCUS OF A MOBILE SITE MEMBRANE

JOHN SANDBLOM, JOHN L. WALKER, JR., *and* GEORGE EISENMAN

From the Department of Physiology and Medical Physics, Biomedical Center, Uppsala, Sweden, the Department of Physiology, The University of Utah, Salt Lake City, Utah 84112, and the Department of Physiology, University of California, Los Angeles, California 90024

ABSTRACT The kinetic properties of a mobile site membrane are analyzed theoretically and the results are compared with experimental data obtained from a simple model system. In the model system the measured response to a step change in electric current is a single relaxation process, in excellent agreement with the theoretically predicted behavior. To this relaxation process corresponds an anomalous capacitance whose properties are obtained by performing a frequency analysis of the system. By plotting the impedance locus of this mobile site membrane, the locus is shown to exhibit a 45° phase angle at high frequencies, a phenomenon which is generally associated with depletion layers.

INTRODUCTION

One approach to understanding the behavior of electrically excitable cell membranes is through the study of artificial or model membranes. It should be possible with simple models, where reasonable assumptions concerning the physics of the model can be made, to describe the model theoretically and then carry out the necessary experiments to test the theory. One particular aspect of this approach is to explain the kinetic properties of a system, i.e., the nature and manifestations of the relaxation processes involved. Most investigations of this problem, however, have been concerned with membranes having fixed boundary concentrations. For these membranes it has been possible to derive theoretical equations predicting the transient (1–3) as well as frequency responses.[1]

Regarding mobile site membranes, Conti and Eisenman (4) published a theory describing the steady-state properties of a membrane with completely dissociated sites and Walker and Eisenman (5) published an experimental confirmation of that theory. Subsequently the kinetic behavior of this system was investigated and the results are presented here. Theoretical equations predicting the transient and frequency responses of the system are derived and compared with the nonsteady-state data obtained during the course of the experiments designed to test the steady-state theory.

[1] Sandblom, J. Manuscript submitted for publication.

THEORY

The membrane consists of two oppositely charged monovalent ions dissolved in a solvent trapped between two boundaries. One of the ions is the mobile site (carrier) and the other is the counterion. The sites cannot cross the boundaries of the membrane but are free to move about within the membrane. The counterions on the other hand can cross the membrane boundaries but because of the restriction imposed by assuming macroscopic electroneutrality they must be present in the membrane in a concentration equal to that of the sites. Both sites and counterions carry current within the membrane. Following the treatment of Nernst and Planck, the fluxes of these two ions within the membrane can be written as shown in equations 1 and 2:

$$J_1(x,t) = -D_1 C_1(x,t) \frac{\partial}{\partial x}\left[\ln C_1(x,t) + z_1 \frac{F}{RT}\psi(x,t)\right], \quad (1)$$

$$J_2(x,t) = -D_2 C_2(x,t) \frac{\partial}{\partial x}\left[\ln C_2(x,t) + z_2 \frac{F}{RT}\psi(x,t)\right]. \quad (2)$$

The subscripts 1 and 2 refer to the sites and counterions, respectively, J is the ion flux (moles per square centimeter per second), D is the diffusion coefficient (square centimeters per second), C is the concentration (moles per cubic centimeter), R is the gas constant (8.317 joules per mole per degree Kelvin), T is the temperature (298.2°K), z is the valence (± 1), F is the Faraday (96,500 coulombs per equivalent), ψ is the electric potential (volts), x is the space coordinate perpendicular to the membrane boundaries (centimeters), and t is time (seconds). We assume macroscopic electroneutrality and therefore $C_1(x, t) = C_2(x, t) = C(x, t)$, making it convenient to drop the subscript from the concentration.

Using the electroneutrality condition and the continuity equations (equation 3) one finds in the usual manner that the two flux equations can be combined to give the diffusion equation as shown in equation 4.

$$\frac{\partial J_i(x,t)}{\partial x} = -\frac{\partial C_i(x,t)}{\partial t}, \quad (3)$$

$$\frac{\partial C(x,t)}{\partial t} = D \frac{\partial^2 C(x,t)}{\partial x^2}, \quad (4)$$

where

$$D = \frac{2D_1 D_2}{D_1 + D_2}. \quad (4a)$$

Equations 5 and 6 are a statement of the fact that the sites cannot cross the bound-

aries and therefore that all of the current is carried by the counterions at the boundaries, $x = 0$ and $x = d$.

$$J_1(0, t) = J_1(d, t) = 0, \tag{5}$$

$$J_2(0, t) = J_2(d, t) = \frac{I}{z_2 F}. \tag{6}$$

In equation 6 I is the current density (amperes per square centimeter). Inserting equations 5 and 6 into equations 1 and 2 we find that

$$\frac{\partial C(0, t)}{\partial x} = \frac{\partial C(d, t)}{\partial x} = -\frac{I}{2 z_2 D_2 F}. \tag{7}$$

In general, the concentration profile within the membrane may have any shape when $t = 0$ but we have limited ourselves to the case where the profile is in the steady-state condition resulting from a maintained constant current density. Conti and Eisenman (4) have shown that under this condition the concentration profile is linear as shown in equations 8 and 9:

$$C(x, 0) = \bar{C}\left[1 + \frac{\phi_1}{d}(2x - d)\right], \tag{8}$$

$$C(x, \infty) = \bar{C}\left[1 + \frac{\phi_2}{d}(2x - d)\right]. \tag{9}$$

$\bar{C}$ is the mean concentration (moles per cubic centimeter) throughout the membrane in the zero current steady-state condition. It has been found convenient to write the current as a function ϕ of the limiting (saturating) current (I_{lim}) for the system as defined by equations 10 *a* and 10 *b*. ϕ_1 is therefore the fraction of limiting current for the steady state at $t = 0$ and ϕ_2 is the fraction of limiting current for the new steady state.

$$\phi = \frac{I}{I_{\text{lim}}}, \tag{10 a}$$

where I_{lim} is given by:

$$I_{\text{lim}} = -\frac{4 F z_1 D_1 \bar{C}}{d}. \tag{10 b}$$

Equation 4 can be solved subject to the conditions of equations 7, 8, and 9 by the method of the Laplace transform, and we shall consider two types of forcing functions: (*a*) a step from fraction of limiting current ϕ_1 to fraction of limiting current ϕ_2, and (*b*) ϕ is a sinusoidal current.

When the step function ϕ is applied at $t = 0$, the solution can be written in the two forms presented as equations 11 and 12 (the method of solution follows the usual procedure for this type of problem, described for example in Carslaw and Jaeger [6]):

$$C(x, t) = \bar{C}\left[1 + \phi_2\left(\frac{2x}{d} - 1\right)\right] - (\phi_1 - \phi_2)\frac{4\bar{C}}{\pi^2}\sum_{n=0}^{\infty}\frac{1}{(2n+1)^2} \cdot 2\cos\left[\frac{(2n+1)\pi x}{d}\right]\exp\left[-\frac{(2n+1)^2\pi^2 Dt}{d^2}\right], \quad (11)$$

$$\begin{aligned} C(x, t) = {} & \bar{C}\left[1 + \phi_2\left(\frac{2x}{d} - 1\right)\right] \\ & - \left(4\phi_1\bar{C}\sqrt{D} + \frac{2\phi_2}{d}\right)\sqrt{\frac{t}{\pi}}\sum_{n=0}^{\infty}(-1)^n \\ & \cdot \left\{\exp\frac{[(n+1)d - x]^2}{4Dt} - \exp\left[-\frac{(nd+x)^2}{d^2}\right]\right\} \\ & + 2\sqrt{D}\left(\phi_1\bar{C} + \frac{\phi_2}{D}\right)\sum_{n=0}^{\infty}(-1)^n \\ & \cdot \left\{\frac{(n+1)d - x}{\sqrt{D}}\operatorname{erfc}\frac{(n+1)d - x}{2\sqrt{Dt}} - \frac{nd+x}{D}\operatorname{erfc}\frac{nd+x}{2\sqrt{Dt}}\right\}. \end{aligned} \quad (12)$$

The infinite series in equation 11 converges rapidly when t is large compared with the time constant $\tau = d^2/\pi^2 D$ while the infinite series in equation 12 converges rapidly when t is small compared with τ.

For the second type of forcing function, we are primarily interested in the solution of equation 4 when $\phi_1 = 0$ and the fraction of limiting current is sinusoidal with a mean of zero as shown in equation 13.

$$\phi = \phi_0 \exp j\omega t, \quad (13)$$

where ϕ_0 is the maximum amplitude and ω is the angular velocity. The solution to equation 4 under these conditions is given by equation 14. Only the undamped periodic terms of the solution are presented because we are not interested in the transient behavior of the system when applying a sinusoidal forcing function.

$$C(x, t) = \bar{C} + \bar{C}\phi\frac{2}{d}\sqrt{\frac{D}{j\omega}}\frac{\sinh\left[\sqrt{\frac{j\omega}{D}}\left(x - \frac{d}{2}\right)\right]}{\cosh\left(\sqrt{\frac{j\omega}{D}}\cdot\frac{d}{2}\right)}. \quad (14)$$

Equation 14 has been obtained by inserting the sinusoidal function of ϕ in equa-

tion 4 which is thereby reduced to a second-order ordinary differential equation. Solving this equation and applying the boundary conditions 7 subsequently yields equation 14.

If we now introduce a quantity z, later to be identified with the impedance, equation 14 can be written in the more convenient form of equation 15:

$$C(x, t) = \bar{C}\,[1 + z\,\phi], \tag{15}$$

where

$$z = \frac{\sinh\left[\alpha\sqrt{j}\left(\frac{2x}{d} - 1\right)\right]}{\alpha\sqrt{j}\cosh\,(\alpha\sqrt{j})}, \tag{16}$$

and

$$\alpha = \frac{d}{2}\sqrt{\frac{\omega}{D}}.$$

Inserting the boundary value $x = d$ in equation 16, and denoting the resulting expression by capital Z, we get

$$Z = \frac{\tanh\,\alpha\sqrt{j}}{\alpha\sqrt{j}} = \frac{\sqrt{2}}{\alpha}\left[\frac{\sin\sqrt{\frac{\alpha}{2}} + \sinh\frac{\alpha}{\sqrt{2}}}{\cos\sqrt{\frac{\alpha}{2}} + \cosh\frac{\alpha}{\sqrt{2}}} + j\,\frac{\sin\frac{\alpha}{\sqrt{2}} - \sinh\frac{\alpha}{\sqrt{2}}}{\cos\frac{\alpha}{\sqrt{2}} + \cosh\frac{\alpha}{\sqrt{2}}}\right]. \tag{17}$$

At $x = 0$ equation 16 assumes the negative value of Z.

To show that Z corresponds to the complex impedance of the membrane we combine equations 1 and 2 and integrate to get

$$IR_\infty = -\frac{RT}{F}\,\frac{D_1 - D_2}{D_1 + D_2}\ln\frac{C(d, t)}{C(0, t)} + V, \tag{18}$$

where

$$R_\infty = \frac{1}{A}\int_0^d \frac{RT\,dx}{F^2(D_1 + D_2)C(x, t)} = \frac{1}{A}\int_0^d \frac{RT\,dx}{F^2(D_1 + D_2)\bar{C}[1 + \phi z]}, \tag{19}$$

and

$$V = \psi\,(d, t) - \psi\,(0, t).$$

Equation 19 defines the instantaneous resistance (ohms) or the resistance at infinite frequency R_∞, and A is the membrane cross-sectional area (square centimeters).

We can now substitute equation 14 (at $x = d$ and $x = 0$ respectively) into equa-

tion 18 which will give the I–V relationship in terms of complex parameters

$$IR_\infty = -\frac{RT}{F}\frac{D_1 - D_2}{D_1 + D_2}\ln\left[\frac{1 + \phi Z}{1 - \phi Z}\right] + V. \tag{20}$$

This is a highly nonlinear expression with respect to ϕ but for small values of ϕ it is possible to expand the expression and retain only first-order terms. The resulting expression for the total impedance dV/dI is then reduced to

$$\frac{dV}{dI} = \frac{RT\,d}{AF^2(D_1 + D_2)\bar{C}}\cdot\left[1 - \frac{D_1 - D_2}{2z_1 D_1}Z\right]. \tag{21}$$

Z therefore represents an impedance function and because of its complex nature which is apparent from equation 17 we may represent it graphically in a phase plane (Fig. 1 *a*). The equivalent circuit which can be inferred from the shape of the impedance locus is also shown (Fig. 1 *b*). It is apparent from this figure that

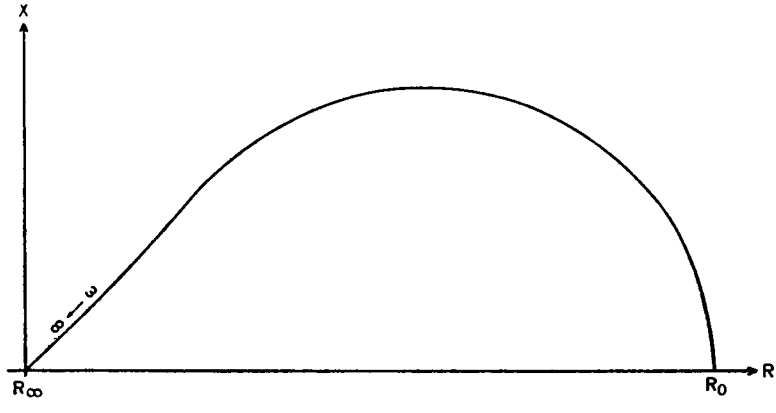

FIGURE 1 *a* Impedance locus calculated from equation 17.

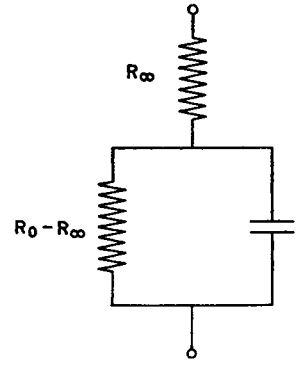

FIGURE 1 *b* The equivalent circuit corresponding to Fig. 1 *a*.

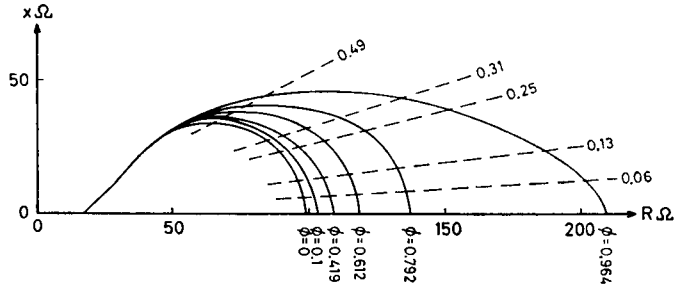

FIGURE 2 Impedance loci ($dV/d\phi$) for different amplitudes ϕ as indicated in the figure. Experimental values for D_1, D_2, d, and A have been used. ($D_1 = 2.0 \cdot 10^{-5}$ cm²/sec, $D_2 = 9.4 \cdot 10^{-5}$ cm²/sec, $d = 5.00$ cm, $A = 2.11 \cdot 10^{-2}$ cm².) The dotted lines connect points of equal (normalized) frequencies as indicated in the figure.

an anomalous reactance in the form of a capacitance is present in the membrane, although the value of the capacitance is strongly frequency dependent in view of the departure from a semicircular locus (Fig. 1 *a*).

Also to be noted is the 45° phase angle at the high-frequency end of the impedance locus which is a characteristic feature of a depletion layer boundary (7, 8). The impedance equation 17 was in fact already derived by Lullies (9) (1937) for an electrolyte layer between two reversible electrodes.

Equation 17 is also obtained from cable theory as the longitudinal impedance of a simple coaxial cable (10). This is the reason why impedance loci of the squid axon (10) have a shape which is very similar to that shown in Fig. 1 *a*.

Fig. 2 shows the effect of increasing the amplitude of the oscillations into the nonlinear region of the system. The curves were obtained by numerical computations. First the periodic function of V corresponding to a sinusoidal current was computed from equations 19 and 20. The maximum values of the V function were then used in calculating the impedance loci shown in Fig. 2. The capacitance of the system is seen to be unaltered as ϕ increases but the low-frequency resistance increases and tends towards infinity as the amplitude reaches the saturation value.

EXPERIMENTAL METHODS FOR TESTING THE STEP RESPONSE OF THE SYSTEM

The experimental system is that described in reference 5. It consists of a 5.0 cm length of polyvinyl (Tygon) tubing (I.D. = 0.164 cm) filled with 0.01 N HCl. The ends are plugged with silver cylinders of 0.17 cm diameter which are used to deliver current. Two silver wires, (0.018 cm diameter) inserted into the lumen of the tubing perpendicular long axis, are used as recording electrodes.

The HCl used for the experiments was prepared by dilution from 5.0 N reagent grade using deionized distilled water. The conductivity of the system was routinely measured at the beginning and at the end of each experiment. Comparison of these measurements showed that there was no significant change in the HCl concentration during the course of any of the experiments.

Before each experiment, the polarizing electrodes were electrolytically coated with enough silver chloride to deliver the desired current for 100 hr. The diameter of these electrodes was slightly larger than that of the lumen of the tubing so a tight mechanical seal was obtained when they were put in place. Final positioning was done under a dissecting microscope with the distance between the two being carefully adjusted to $d = 5.00 \pm 0.02$ cm.

The recording electrodes were placed at the points $a = 0.04d$ and $b = 0.96d$. Once in place they were chlorided in 0.1 N HCl and then rinsed with deionized distilled water. After the membrane was assembled one of the electrodes was grounded and used as the reference electrode for potential measurements. The other electrode was connected to the input of a Cary Model 21 vibrating reed electrometer (Cary Instruments, Monrovia, Calif.). The output of the electrometer was intermittently read directly while being recorded continuously on a Rustrak strip chart recorder (Rustrak Instrument Div., Gulton Industries, Inc., Manchester, N. H.) with a chart speed of 1 inch/hr.

The tubing, with the silver electrodes and necessary lead wires, was placed in a polyethylene bag which was then immersed in a constant temperature (25.0 ±0.2°C) water bath.

Constant electric current was delivered through the polarizing electrodes from nickel-cadmium batteries (isolated from ground) in series with a calibrated resistor having at least 100 times the maximum resistance of the "membrane" at any time. The current was monitored intermittently during the experiments by measuring the voltage drop across a second, smaller series resistor of value calibrated to within ±0.05%. The batteries were found to deliver very stable currents over long time periods (weeks) with the small currents used for the experiments.

The ratio of the chloride activities at the two recording electrodes was measured periodically by turning the current off for 3–4 sec and reading the zero current potential. As can be seen from the time constant of the system these brief interruptions were of no consequence.

For a more detailed description of the experimental system, see Walker and Eisenman (1966) (5).

RESULTS

The experimental results are presented in Figs. 3 and 4. Fig. 3 shows the increase of the concentration potential $V_{a,b}^{obs0}$ measured between the two recording electrodes with time for five different values of ϕ. Fig. 4 shows, for the same experiments, the decrease of the potential with time as the concentration profile relaxes after the current has been turned off. In both figures, the dots are experimental points and the lines are theoretical curves calculated from:

$$V_{a,b}^{obs0} = -2t_H \frac{RT}{F} \ln \frac{C(b)}{C(a)},$$

where $C(b)$ and $C(a)$ have been calculated from equation 11. Because of the rapid convergence of the infinite series in equation 11, only four terms were used to calculate the point at 1 hr, and after 10 hr only one term was used. The values of t_H, D_1, and D_2 were taken from the literature.

The agreement between the theoretically predicted and the experimentally obtained behavior is seen to be quite satisfactory. This simple system therefore be-

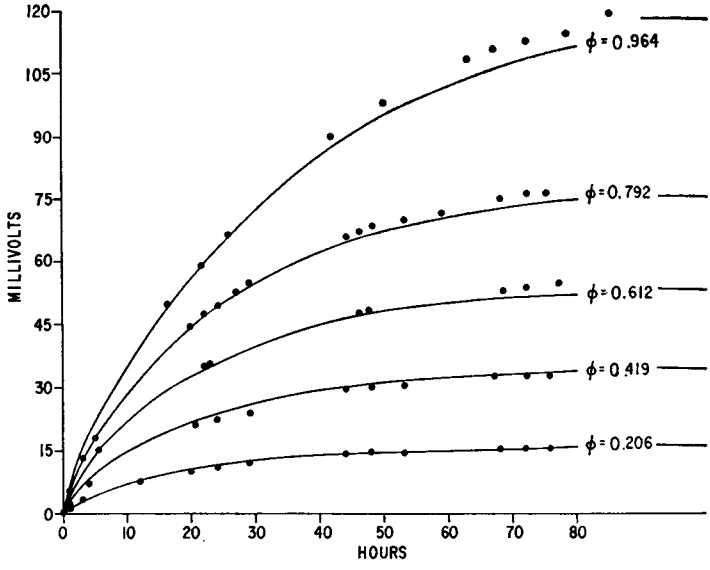

FIG. 3 The concentration potential between *a* and *b* is plotted as a function of time after the onset of an applied electric current. Points are experimental and lines are theoretical.

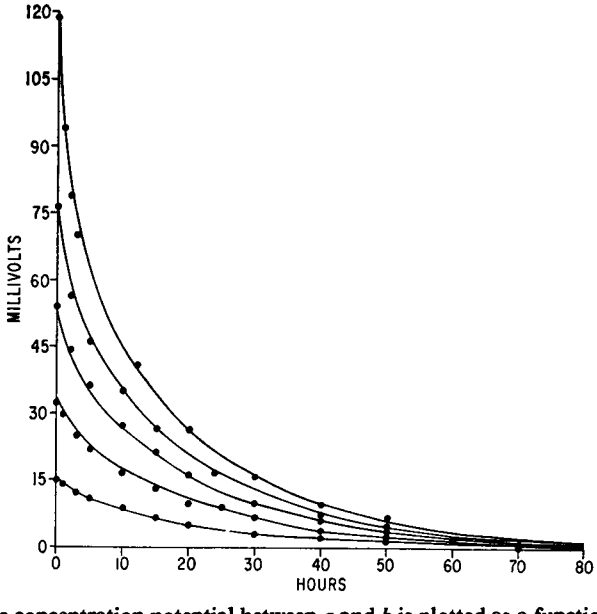

FIGURE 4 The concentration potential between *a* and *b* is plotted as a function of time after the interruption of an applied electric current. Points are experimental and lines are theoretical.

haves like an ideal mobile site membrane with respect to steady-state as well as nonsteady-state properties. It also follows that it possesses an *anomalous capacitative reactance*, whose magnitude will depend on the diffusion parameters according to equation 17.

DISCUSSION

We have shown that a simple experimental model of a mobile site membrane conforms to the electrodiffusion equations when the condition of trapped sites is introduced. Since such mobile sites may be considered as carriers, we may infer from the behavior of the membrane studied here some of the properties associated with carrier transport. Of particular interest is the large anomalous reactance in the form of a capacitance which was shown to be dependent on the diffusion parameters but independent of the electric field. The 45° phase angle exhibited by the impedance locus is characteristic of mobile site membranes which may be viewed as electrodiffusion regimes containing depletion layers for which this property has previously been demonstrated (7, 9).

We wish to thank Dr. Michael Fox for writing the computer program and making the calculations shown in Fig. 2.

This work was supported by National Science Foundation grant GB-4039, and U.S. Public Health Service grants GM-14404 and FR-5367.

Received for publication 3 December 1970.

REFERENCES

1. MAURO, A. 1962. *Biophys. J.* **2**:179.
2. COHEN, H., and J. COOLEY. 1965. *Biophys. J.* **5**:145.
3. COLE, K. S. 1965. *Physiol. Rev.* **45**:340.
4. CONTI, F., and G. EISENMAN. 1966. *Biophys. J.* **6**:227.
5. WALKER, J., and G. EISENMAN. 1966. *Biophys. J.* **6**:513.
6. CARSLAW, H., and J. JAEGER. 1947. Conduction of Heat in Solids. The Clarendon Press, Oxford, England.
7. WARBURG, E. 1899. *Ann. Phys. Chem.* **67**:493.
8. BUCK, R. P. 1968. *J. Electroanal. Chem.* **18**:381.
9. LULLIES, H. 1937. *Biol. Rev. (Cambridge).* **12**:338.
10. COLE, K. S. 1968. Membranes, Ions and Impulses. University of California Press, Berkeley.